

Strain-Induced Splitting and Oscillator-Strength Anisotropy of the Infrared Transverse-Optic Phonon in Calcium Fluoride, Strontium Fluoride, and Barium Fluoride

Albert Feldman and Roy M. Waxler

National Bureau of Standards, Washington, D. C. 20234

(Received 21 January 1980)

Strain-induced splittings of the infrared-active TO phonon in CaF_2 , SrF_2 , and BaF_2 are calculated from a least-squares fit of photoelastic dispersion data by an undamped oscillator model. The strain-induced oscillator-strength anisotropy appears negligible; the Szigeti effective charge remains a scalar. The shear deformation potential for [100] strain is $\sim 170 \text{ cm}^{-1}$ in all the materials; for [111] strain it is -82 cm^{-1} for CaF_2 , -54 cm^{-1} for SrF_2 , and -50 cm^{-1} for BaF_2 .

PACS numbers: 63.20.Dj, 71.70.Ej, 78.20.Fm, 78.30.Gt

The effect of uniaxial stress on the lattice absorption bands of ionic materials has been difficult to study because of the relatively broad bandwidth of the absorption spectra and the difficulty of applying large stresses to extremely thin specimens. In contrast, the study of uniaxial stress effects on the Raman spectra of solids¹ has been facilitated by the sharp nature of the spectra and the ability to use bulk specimens. There have been significant studies of the effects of hydrostatic pressure on the transverse-optic (TO) phonon of a wide range of thin-film halide materials² that have yielded the transverse-optic-mode Grüneisen parameter, γ_{TO} . Furthermore, a large body of literature has related the effect of hydrostatic pressure on the static dielectric constant ϵ_0 , and the high-frequency dielectric constant ϵ_∞ , to γ_{TO} and to the volume dependence of the Szigeti effective charge e_s .³ While it would be desirable to measure directly the effect of uniaxial strain on absorption due to the TO-phonon mode, it is the purpose of this paper to show that this effect can be determined indirectly from the measurement of the infrared dispersion of the photoelastic constants of ionic materials. We present photoelastic constant data derived from piezobirefringence studies on the alkaline-earth

materials CaF_2 , SrF_2 , and BaF_2 ; and, based on a least-squares fit of the data by an oscillator model, we derive values for the strain-induced splitting of the TO-phonon mode and the strain-induced anisotropy of the oscillator strength. This information, in conjunction with the results of nonlinear elastic-constant measurements and stress-Raman measurements, will provide input for the development of models of fluorite-structure anharmonic potentials and for the validation of such models. The data we present are the first systematic determination of photoelastic-constant dispersion in the infrared due to lattice vibrations. Furthermore, to our knowledge, this is the first determination of infrared TO-mode splitting due to uniaxial stress in an ionic material whose infrared-active mode is Raman forbidden.

Recently, Humphreys and Maradudin⁴ (HM) and Bendow, Gianino, Tsay, and Mitra⁵ have presented phenomenological expressions for the photoelastic constants k_{ijkl} in the infrared region of the spectrum. Using both experimental data and models for interionic potentials and dipole moments, they have calculated phenomenological parameters for a wide range of zinc-blende and alkali-halide crystals. Subsequently, several ex-

TABLE I. Tensor components in contracted notation for strain birefringence due to [100] and [111] strain.

Strain	k^∞	g	h
[100]	$k_{11}^\infty - k_{12}^\infty$	$g_{11} - g_{12} = \frac{\partial G_1}{\partial \eta} - \frac{\partial G_2}{\partial \eta}$	$h_{11} - h_{12} = -\frac{2G_0(a' - b')}{\nu_{\text{TO}}}$
[111]	k_{44}^∞	$g_{44} = \frac{\partial G_1}{\partial \eta} - \frac{\partial G_2}{\partial \eta}$	$h_{44} = -\frac{2G_0 c'}{\nu_{\text{TO}}}$

periments were conducted that suggested inadequacies in these models.^{6,7} However, the experimental data were obtained at few wavelengths and were prone to large experimental errors, and, hence, did not provide a stringent test of the models. In this paper, we show that the basic phenomenological expressions agree quite well with our data on the alkaline-earth fluorides.

The dielectric tensor of a cubic ionic material in the infrared can be represented in the harmonic approximation by a single undamped oscillator equation of the form

$$\epsilon_{ij}(\nu) = \delta_{ij}\epsilon_{\infty} + G_{ij}/[1 - (\nu/\nu_{\text{TO}})^2], \quad (1)$$

where ν is the angular frequency of the radiation, ν_{TO} is the frequency of the TO phonon, and $G_{ij} = G_0\delta_{ij}$ is the oscillator strength tensor which is related to the density, the transverse effective charge, and the reduced mass of the crystal basis. If the crystal undergoes a small strain η_{kl} , then k_{ijkl} can be represented by

$$k_{ijkl} = k_{ijkl}^{\infty} + \frac{g_{ijkl}}{1 - (\nu/\nu_{\text{TO}})^2} + \frac{h_{ijkl}(\nu/\nu_{\text{TO}})^2}{[1 - (\nu/\nu_{\text{TO}})^2]^2}, \quad (2)$$

where $k_{ijkl} = \partial\epsilon_{ij}/\partial\eta_{kl}$, $g_{ijkl} = \partial G_{ij}/\partial\eta_{kl}$, and h_{ijkl} is related to the strain-dependent TO-mode frequency splitting; the g and h tensors can be related, simply, to the a and b tensors of HM.⁴ If the strain is uniaxial along either the [100] axis or the [111] axis, the TO phonon splits into two levels, and the crystal becomes uniaxial. The photoelastic constants that describe the strain-induced birefringence are given by

$$k = k^{\infty} + \frac{g}{1 - (\nu/\nu_{\text{TO}})^2} + \frac{h(\nu/\nu_{\text{TO}})^2}{[1 - (\nu/\nu_{\text{TO}})^2]^2}, \quad (3)$$

where k , k^{∞} , g , and h are defined in Table I, which employs a contracted notation.⁸ In the table, the terms $a' - b'$ and c' are the shear deformation potentials or the induced splittings per unit strain of the TO phonon due to [100] and [111] strains, respectively. They can be derived by the use of group theory in a manner analogous to the derivation of the a , b , and c deformation-potential parameters of the strain-induced Raman splitting.⁹

The piezobirefringence coefficients $q_{11} - q_{12}$ and q_{44} of CaF_2 , BaF_2 , and SrF_2 have been measured at room temperature over the wavelength range 0.45 to 10.6 μm by a static-stress method. A compensator technique¹⁰ has been used with a procedure modification, described below, to enhance the sensitivity to the small retardations obtained in the infrared. The experimental ar-

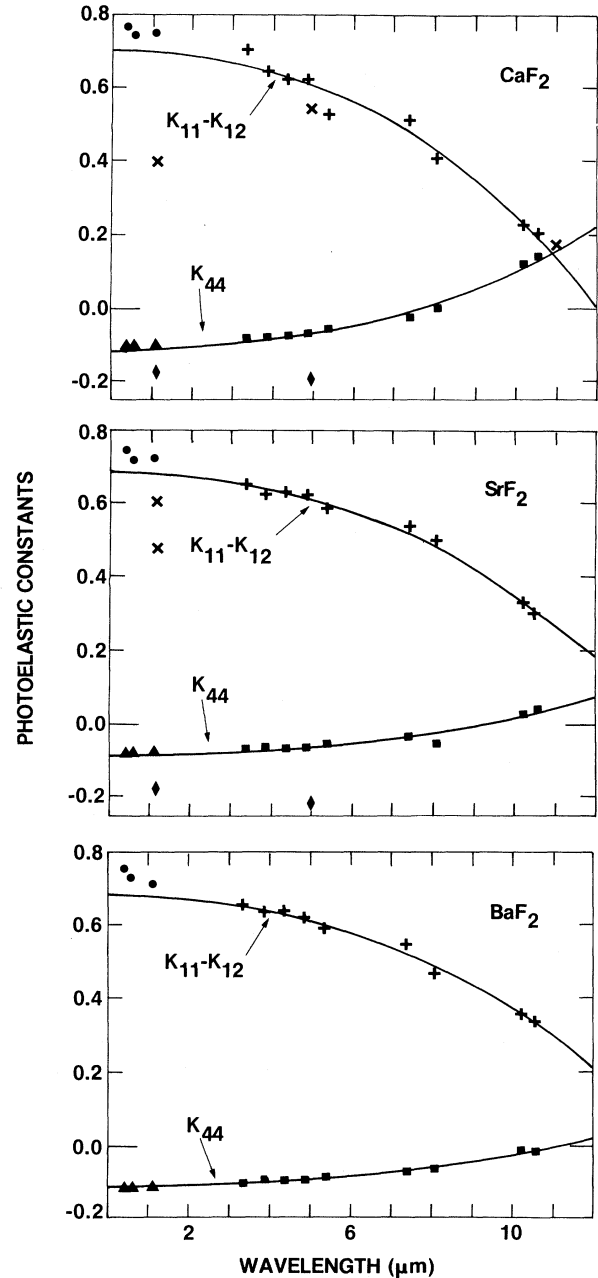


FIG. 1. Photoelastic constants of CaF_2 , SrF_2 , and BaF_2 derived from piezobirefringence data. The curves are least-squares fits by Eq. (3) of the data points denoted by pluses for $k_{11} - k_{12}$ and squares for k_{44} . The circles and triangles represent our data that were not used in the fit. The crosses and diamonds are data derived from the literature (Ref. 6) with a sign reversal on the data k_{44} data to provide better agreement with our data.

angement consisted of an appropriately oriented polarizer, specimen, compensator, analyzer, and detector placed sequentially in a monochro-

matic beam. A reading of the output intensity was noted after the compensator, consisting of a plate of Ge or SiO₂ in a calibrated load cell, was set initially to a quarter-wave retardation. A known uniaxial load was now applied to the specimen, changing the intensity reading, whereupon the stress on the compensator was changed to return the intensity reading to its initial value. From the known loads on the specimen and compensator, we computed the piezobirefringence coefficient. The procedure was then repeated with the compensator set initially to a three-quarter-wave retardation, and an average of the computed coefficients was taken. The two measurements compensate for possible systematic intensity changes.

The photoelastic constants $k_{11} - k_{12}$ and k_{44} were calculated and plotted as shown in Fig. 1. We also calculated $k_{11} - k_{12}$ and k_{44} of CaF₂ and SrF₂ from data obtained by other workers.⁶ We believe their data to be questionable because their sign for k_{44} is opposite in sign to values for the visible in the published literature^{11,12} which agree with our sign; even if we reverse the sign of their k_{44} , these values and their values for $k_{11} - k_{12}$ at 1.15 μm do not fit smoothly to known visible and ultraviolet dispersion data.¹² (In Fig. 1, we show their data with the sign of k_{44} reversed, superimposed on our data.)

An important feature of our data is the strong infrared dispersion which produces a sign change in k_{44} of CaF₂ and SrF₂ at the longer wavelengths. In order to obtain a theoretical model for this dispersion, the data from 3.4 to 10.6 μm were fitted by Eq. (3) by the method of least squares and values for the parameters k^∞ , g , and h were obtained. The resulting curves are shown in Fig. 1 superimposed on the experimental data; the fit

appears to be quite good. The shorter wavelength data were omitted from the fit because accurate refractive index data on these materials had indicated that dispersion due to electronic processes is still significant at these wavelengths.

The principal results of the statistical fit are values for the stress-induced oscillator-strength anisotropies, $g_{11} - g_{12}$ and g_{44} , and values for the TO-mode shear-deformation potentials $a' - b'$ and c' , which are shown in Table II. The parameters used for calculating the frequency splittings, G_0 , and ν_{TO} were obtained from accurate refractive-index data,¹³⁻¹⁵ rather than from the experimental parameters derived from infrared reflectivity measurements.¹⁴ This approach is reasonable because the infrared reflectivity data show that the lattice absorption comes predominantly from a single oscillator, the TO mode, and secondarily from a much weaker oscillator, a combined TO-acoustic mode. Moreover, at frequencies far from any of these resonances, one can consider the refractive-index dispersion as due to a single undamped oscillator, analogous to the Penn oscillator model¹⁶ for electronic transitions. Finally, a single oscillator composite of two oscillators, to lowest order, obeys the condition

$$G_0 \nu_0^2 = G_1 \nu_1^2 + G_2 \nu_2^2, \quad (4)$$

where G_0 is the oscillator strength of the composite oscillator, ν_0 is its resonant frequency, G_1 and G_2 are the oscillator strengths of the individual oscillators, and ν_1 and ν_2 are their respective resonance frequencies. The oscillator parameters we have used are reasonable because their values, given in Table II, and the parameters of Kaiser *et al.*¹⁷ obey Eq. (4) quite well. If the TO-mode parameters of Kaiser *et al.* are used to

TABLE II. Shear deformation potential and strain-induced oscillator-strength anisotropy of the infrared TO phonon in CaF₂, SrF₂, and BaF₂.

	CaF ₂	SrF ₂	BaF ₂
G_0	3.85 ^a	3.35 ^b	3.83 ^c
ν_{TO} (cm ⁻¹)	289 ^a	251 ^b	213 ^c
ν_{Raman} (cm ⁻¹)	327 ^d	...	247 ^d
$g_{11} - g_{12}$	0.00 ± 0.06	0.00 ± 0.03	0.00 ± 0.03
g_{44}	0.00 ± 0.02	0.00 ± 0.03	0.00 ± 0.01
$a' - b'$ (cm ⁻¹)	169 ± 12	171 ± 7	174 ± 8
$a - b$ (cm ⁻¹) (Raman)	-1016 ^d	...	-504 ^d
c' (cm ⁻¹)	-82 ± 4	-54 ± 6	-50 ± 3
c (cm ⁻¹) (Raman)	-103 ^d

^aRef. 13.

^bRef. 14.

^cRef. 15.

^dRef. 9.

compute the deformation potentials, the values obtained would differ by less than 8%.

For comparison, we show in Table II shear deformation potentials for the Raman-active modes in CaF_2 and BaF_2 .⁹ The values of $a' - b'$ are significantly smaller in magnitude and opposite in sign to the corresponding values for $a - b$. On the other hand, c and c' in CaF_2 are of comparable value and we find $c'/\nu_{\text{TO}} \approx c/\nu_{\text{Raman}}$. We have also found that for CaF_2 and BaF_2 , the shear deformation potentials are much smaller than the hydrostatic deformation potentials, $a' + 2b'$, computed from the TO-mode Grüneisen parameters.^{18, 19}

The principal conclusions we can draw from the fit are these: The stress-induced anisotropy in the oscillator strength is indistinguishable from zero in all cases, indicating that the Szigeti effective charge e_s remains a scalar; the shear deformation parameter $a' - b'$ does not vary, within experimental error, from material to material; c' is opposite in sign to $a' - b'$ and its values for SrF_2 and BaF_2 are equal within experimental error, but are significantly smaller than the value for CaF_2 . Work is planned for the development of a microscopic model of the fluorite structure to explain these results.

This work was supported in part by the Air Force Office of Scientific Research, Air Force Systems Command, U. S. Air Force, under Grants No. AFOSR-ISSA-79-0001 and No. AFOSR-ISSA-80-00002.

¹V. J. Tekippe and A. K. Ramdas, Phys. Lett. **35A**, 143 (1971).

²R. P. Lowndes and A. Rastogi, Phys. Rev. B **14**, 3598 (1976).

³A recent example is J. Shanker, V. P. Gupta, and O. P. Sharma, Phys. Rev. B **18**, 5869 (1978).

⁴L. B. Humphreys and A. A. Maradudin, Phys. Rev. B **6**, 3868 (1972).

⁵B. Bendow, P. D. Gianino, Y. F. Tsay, and S. S. Mitra, Appl. Opt. **13**, 2382 (1974).

⁶J. P. Szczesniak, D. Cuddback, and J. C. Corelli, J. Appl. Phys. **47**, 5356 (1976).

⁷A. Feldman, D. Horowitz, and R. M. Waxler, Appl. Opt. **16**, 2925 (1977).

⁸J. F. Nye, *Physical Properties of Crystals* (Oxford Univ. Press, London, 1957), pp. 243-254.

⁹S. Venugopalan and A. K. Ramdas, Phys. Rev. B **8**, 717 (1973).

¹⁰A. Feldman, Opt. Eng. **17**, 453 (1978).

¹¹K. V. Rao and T. S. Narasimhamurthy, J. Phys. Chem. Solids **31**, 876 (1970).

¹²C. Sanchez and M. Cardona, Phys. Status Solidi B **50**, 293 (1972).

¹³I. H. Malitson, Appl. Opt. **2**, 1103 (1963).

¹⁴M. J. Dodge, in *Laser Induced Damage in Optical Materials: 1978*, U. S. National Bureau of Standards Special Publication No. 541, edited by A. J. Glass and A. H. Guenther (U.S. GPO, Washington, D.C., 1979), p. 55.

¹⁵I. H. Malitson, J. Opt. Soc. Am. **54**, 628 (1964).

¹⁶D. Penn, Phys. Rev. **128**, 2093 (1962).

¹⁷W. Kaiser, W. G. Spitzer, R. H. Kaiser, and L. E. Howarth, Phys. Rev. **127**, 1950 (1962).

¹⁸R. P. Lowndes, J. Phys. C. **4**, 3083 (1971).

¹⁹J. R. Ferraro, H. Horan, and A. Quattrochi, J. Chem. Phys. **55**, 664 (1971).